The EMBO Journal Vol. 22 No. 1 pp. 151–163, 2003

Structure of the topoisomerase VI-B subunit: implications for type II topoisomerase mechanism and evolution

Kevin D.Corbett and James M.Berger[1]

Department of Molecular and Cellular Biology, University of California, Berkeley, 327 Hildebrand Hall 3206, Berkeley, CA 94720, USA

[1]Corresponding author
e-mail: jmberger@uclink4.berkeley.edu

Type IIA and type IIB topoisomerases each possess the ability to pass one DNA duplex through another in an ATP-dependent manner. The role of ATP in the strand passage reaction is poorly understood, particularly for the type IIB (topoisomerase VI) family. We have solved the structure of the ATP-binding subunit of topoisomerase VI (topoVI-B) in two states: an unliganded monomer and a nucleotide-bound dimer. We find that topoVI-B is highly structurally homologous to the entire 40–43 kDa ATPase region of type IIA topoisomerases and MutL proteins. Nucleotide binding to topoVI-B leads to dimerization of the protein and causes dramatic conformational changes within each protomer. Our data demonstrate that type IIA and type IIB topoisomerases have descended from a common ancestor and reveal how ATP turnover generates structural signals in the reactions of both type II topoisomerase families. When combined with the structure of the A subunit to create a picture of the intact topoisomerase VI holoenzyme, the ATP-driven motions of topoVI-B reveal a simple mechanism for strand passage by the type IIB topoisomerases.
Keywords: allostery/archaea/ATPase/DNA-binding protein/topoisomerase

Introduction

DNA topoisomerases are a broad group of enzymes with the ability to manipulate the topological state of DNA. Through a complicated and still incompletely understood series of DNA breakage and rejoining steps, these enzymes can perform various reactions on DNA including decatenation, unknotting and modulation of superhelicity. DNA topoisomerases fall into two general classes, type I and type II, which are distinguished by their ability to cleave one or both strands of a DNA duplex, respectively (for reviews, see Wang, 1996, 2002; Champoux, 2001).

Type II topoisomerases carry out strand passage by first generating a transient double-strand (ds) DNA break in a 'gate' or G-segment through nucleophilic attack on the DNA backbone and the formation of 5′-phosphotyrosyl enzyme–DNA linkages. The broken G-segment ends are then separated, a second duplex (the 'transfer', or T-segment) passed through the break, and the broken G-segment duplex resealed. The type II topoisomerase reaction is coupled to ATP binding and hydrolysis, which coordinates the sequential opening and closing of enzyme 'gates' that drive G-segment separation and T-segment transport (Roca and Wang, 1992, 1994).

Type II topoisomerases can be divided into two subclasses: type IIA and type IIB (Bergerat *et al*., 1997; Nichols *et al*., 1999). The type IIA enzymes are the predominant form and are found in some bacteriophages, viruses and archaea, and in all bacteria and eukaryotes. All type IIA topoisomerases are related to each other at the amino acid sequence level, though their oligomeric organization sometimes differs. For example, microbial type IIA topoisomerases are A_2B_2 heterotetramers, while the eukaryotic enzymes are homodimers of a B-A subunit fusion protein (Figure 1A). Catalytic functions within the type IIA enzymes are arrayed in a modular fashion, with the ATPase site located in the B region and the DNA binding/cleavage activity formed from domains in the B and A regions (Figure 1A).

Type IIB topoisomerases comprise a much smaller group than the type IIA enzymes, with topoisomerase VI as the sole representative of the family (Champoux, 2001). Topoisomerase VI enzymes are A_2B_2 heterotetramers found principally in archaea, though recent evidence has shown that they also exist in plants (Hartung and Puchta, 2001; Hartung *et al*., 2002; Sugimoto-Shirasu *et al*., 2002; Yin *et al*., 2002). The topoisomerase VI A subunit (topoVI-A) shares sparse sequence similarity with the type IIA topoisomerases, principally in a region required for DNA cleavage known as a 'toprim' domain (Aravind *et al*., 1998; Nichols *et al*., 1999). However, topoVI-A is not homologous to regions of type IIA enzymes outside the toprim domain, and instead shares general homology with Spo11, a protein responsible for creating dsDNA breaks to initiate meiotic recombination (Keeney *et al*., 1997; Celerin *et al*., 2000; Martini and Keeney, 2002). Indeed, the similarity between topoVI-A and Spo11 helped prove that the A subunit of type IIB topoisomerases contains the DNA binding and cleavage activities, and further, allowed identification of the active site tyrosine responsible for DNA cleavage (Bergerat *et al*., 1997). The only region of the topoisomerase VI B subunit (topoVI-B) held in common with type IIA enzymes at the amino acid sequence level is an ~200 amino acid domain at its N-terminus that is homologous to the GHKL-type ATPases, a large family that also includes MutL, Hsp90 and CheA proteins (Bergerat *et al*., 1997; Dutta and Inouye, 2000).

Since only sporadic sequence motifs are shared between the two type II topoisomerase families (Figure 1A), it has remained unclear whether type IIA and IIB enzymes are remote cousins of each other or represent distinct type II topoisomerase sub-classes. Structural studies of type IIB topoisomerases to date have only deepened this question. The structure of topoVI-A from *Methanococcus*

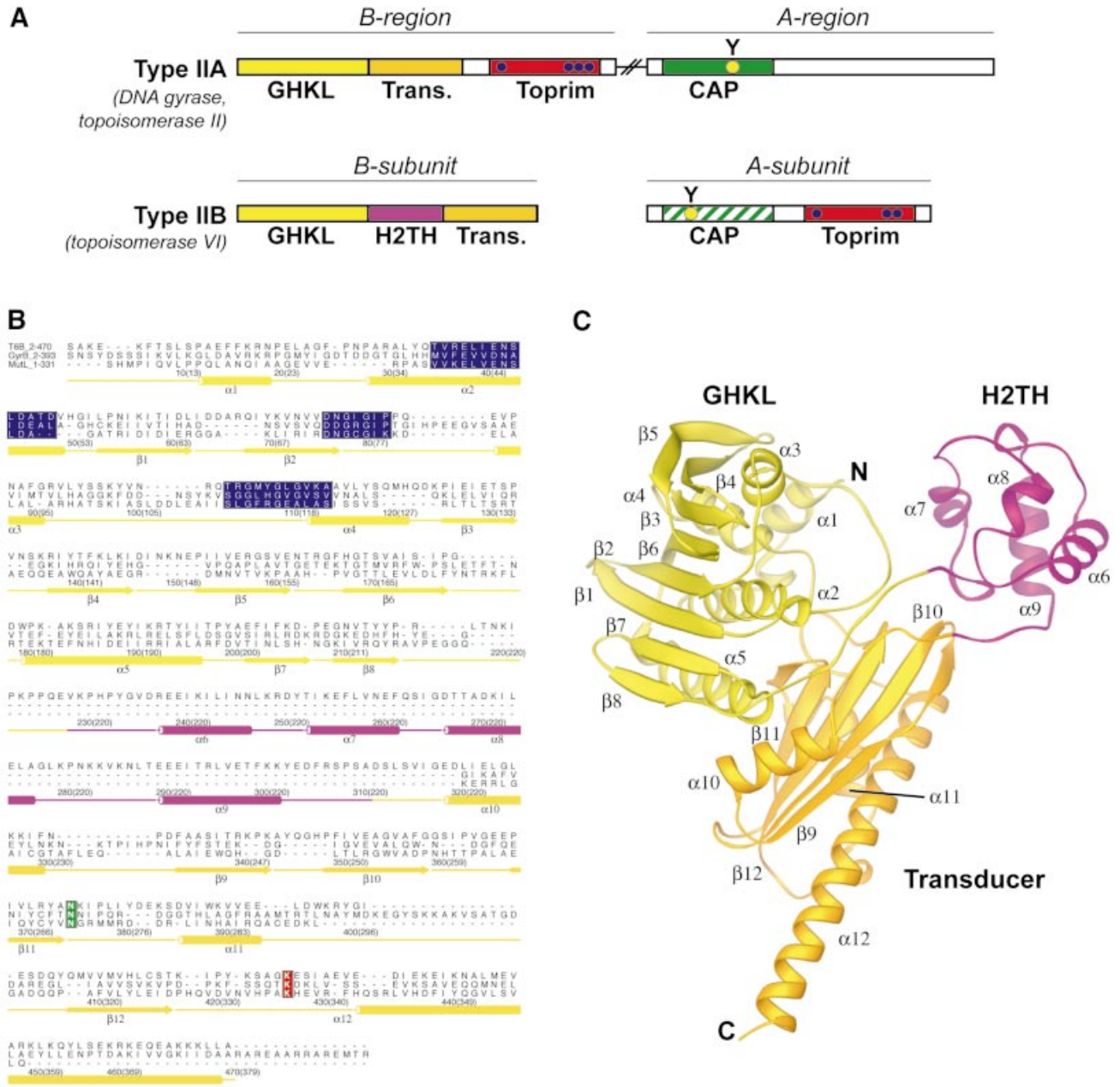

Fig. 1. TopoVI-B′ monomer. (**A**) Domain organization of type II topoisomerases. Key functional modules of type IIA and IIB topoisomerases are labeled as follows: GHKL (yellow), CAP (green) and toprim (red). A conserved 'transducer' domain (Trans.) is shown in orange and the H2TH domain of topoVI-B′ is shown in pink. The split of the A and B regions in prokaryotic type IIA enzymes into discrete subunits is indicated by the double hash mark. The active-site tyrosines (yellow circles) are labeled as 'Y' and conserved acidic residues within the toprim fold are shown as blue circles. While the GHKL and toprim folds of type IIB topoisomerases are identifiable by sequence homology, the type IIB CAP region (striped green) has no sequence homology to the equivalent fold in type IIA proteins. Furthermore, the N- to C-terminal orientation of the CAP and toprim modules is swapped between the two type II topoisomerase families. (**B**) Structure-based sequence alignment of topoVI-B′ with the ATPase regions of *E.coli* GyrB and MutL. The secondary structural elements of topoVI-B′ are shown below the sequences. The three domains are colored as in (A). Residue numbering is that of topoVI-B′ followed by that of GyrB in parentheses. Highlighted in blue are the GHKL motifs identified by Bergerat *et al*. (1997). Highlighted in red is the invariant lysine (427 in topoVI-B′, 337 in GyrB) that contacts the γ-phosphate of bound nucleotide and highlighted in green is a highly conserved asparagine (375 in topoVI-B′, 271 in GyrB) that serves as an anchoring element between the GHKL and transducer domains. (**C**) Structure of the monomer (apo) form of topoVI-B′. Domains are colored as in (A). Secondary structural elements are labeled as in (B). (B) was generated by ALSCRIPT (Barton, 1993) and (C) with RIBBONS (Carson, 1991).

jannaschii revealed that, in addition to the conserved toprim domain, the A subunit contains a helix–turn–helix fold of the catabolite activator protein (CAP) family of DNA-binding proteins, and that the active site tyrosine responsible for DNA cleavage resides on this domain (Nichols *et al*., 1999). In type IIA topoisomerases, the active site tyrosine is also located on a CAP fold (Berger *et al*., 1996), though on a different secondary structural element than in topoVI-A (Nichols *et al*., 1999). In order to maintain proper active site architecture, the positioning of

the toprim and CAP domains is different in type IIB and type IIA topoisomerases, resulting in globally different subunit structures in the two enzyme families. The presence of the CAP and toprim domains in topoVI-A indicates that the DNA cleavage mechanisms of type IIA and type IIB topoisomerases are chemically similar. However, the major structural differences between the two families' DNA binding and cleavage subunits have left their evolutionary kinship open to debate.

Ancestry aside, the physical mechanism by which type IIB topoisomerases pass one DNA duplex through another has likewise remained unresolved. The architecture of topoVI-A initially indicated that the G-segment would lie across the A subunit dimer interface, and that the two halves of the A subunit dimer would separate during G-segment opening to allow T-segment transport (Nichols *et al*., 1999). This model, combined with the observation that the GHKL domains of type IIA topoisomerases and MutL proteins dimerize upon nucleotide binding (Wigley *et al*., 1991; Ali *et al*., 1995; Ban *et al*., 1999), suggested that the B subunits might act as a nucleotide-dependent gate to 'bridge' the cleaved G-segment while the A subunit dimer was separated. The model further predicted that since strand passage is ATP dependent, the B subunits would physically transmit nucleotide-dependent conformational signals to the A subunits that would guide their separation to allow T-segment exit. It has not been demonstrated, however, whether the GHKL folds of the topoVI-B subunits self-associate in response to nucleotide binding, nor has it been shown how these subunits communicate with the A subunits.

To address these mechanistic questions and to clarify the ancestral relationship of the type IIA and type IIB topoisomerases, we determined the three-dimensional structure of a truncated form of topoVI-B, both free and complexed to the ATP analog adenosine [β,γ-imido]triphosphate (AMP-PNP). Unexpectedly, our data reveal that topoVI-B is structurally homologous to the entire 40–43 kDa ATPase region of type IIA topoisomerases and MutL proteins. TopoVI-B contains not only an ATP-binding GHKL module, but also a domain that is known to be important in nucleotide hydrolysis and the transduction of structural signals from the ATP-binding site to the DNA breakage/reunion regions of these enzymes. Our data show that topoVI-B dimerizes in response to ATP binding and undergoes significant interdomain rearrangements centered about the active site pocket, which together explain how ATP stimulates G-segment cleavage and opening by the topoVI-A subunits. This work demonstrates that the type IIA and IIB topoisomerases are directly related evolutionarily, and that the nucleotide-dependent switching elements of GHKL ATPases are conserved.

Results

Apo structure

During purification of the 530 amino acid full-length *Sulfolobus shibatae* topoVI-B subunit, a contaminating species was observed to co-purify with the full-length product. Mass spectrometry identified this protein as a proteolyzed fragment of topoVI-B that ended at amino acid 470. This truncation (topoVI-B′) was subsequently cloned, purified and crystallized without nucleotide in the space group $P2_12_12$, with one protein monomer per asymmetric unit. The structure was solved to 2.0 Å resolution using multi-wavelength anomalous dispersion methods (MAD) with selenomethione-labeled protein. All residues in the final model were traceable directly from the solvent-flattened, experimentally determined electron density maps. The final model includes amino acids 10–96 and 98–470, and was refined to an *R*-factor of 21.4% and an R_{free} of 23.9% (Table I).

The topoVI-B′ protomer contains three domains (Figure 1C). The N-terminal domain (amino acids 10–229) consists of an eight-stranded mixed β-sheet backed on one side by five α-helices. The fold, as anticipated, belongs to the GHKL family of ATPases, which includes MutL, Hsp90, CheA-type histidine kinases and type IIA topoisomerases (Bergerat *et al*., 1997; Dutta and Inouye, 2000). The structure of this domain is particularly similar to the GHKL domain of *Escherichia coli* gyrase B (GyrB) (Wigley *et al*., 1991), a type IIA topoisomerase. The C_α r.m.s.d. between the GHKL regions of topoVI-B′ and GyrB is 1.17 Å for 112 core residues (Figure 2A), despite <15% overall sequence identity between the domains. Within the GHKL domain, one loop (residues 95–98) near the putative nucleotide-binding pocket is disordered. This loop is in a more 'open' conformation than the equivalent loop of AMP-PNP-bound GyrB, and becomes ordered upon nucleotide binding (see below).

The second domain of topoVI-B′ appears as an insertion between the N- and C-terminal domains, and is attached to these regions by 9- to 12-amino acid linker peptides that stretch across the edge of the N-terminal/C-terminal domain interface. The core of the second domain consists of four α-helices, which create a fold that is structurally related to a segment from the formamidopyrimidine-DNA glycosylase (Fpg)/endonuclease VIII (endoVIII) family of DNA base excision repair proteins. This fold is known as a helix–two turns–helix (H2TH) motif (Figure 2B; Sugahara *et al*., 2000; Zharkov *et al*., 2002). In Fpg, the H2TH motif was initially proposed to bind DNA because of its structural similarity to DNA-binding domains such as the helix–hairpin–helix and the helix–three turns–helix motifs (Sugahara *et al*., 2000). However, several recent structures of Fpg/endoVIII family glycosylases bound to DNA have revealed that the H2TH domains of these proteins are only peripherally involved in binding DNA. Rather, their primary function may be simply to position the N-terminal lobe and C-terminal zinc finger domain of the glycosylases for interactions with DNA (Fromme and Verdine, 2002; Gilboa *et al*., 2002; Serre *et al*., 2002; Zharkov *et al*., 2002). Although the H2TH domain appears to be retained in all archaeal and plant type IIB topoisomerases identified to date, it has no known function and has not been observed in other topoisomerase families.

The third domain of topoVI-B′ is a four-stranded β-sheet backed by three α-helices, the last of which is >50 amino acids long and extends from the body of the protein by several turns. Unexpectedly, this domain is structurally related to the C-terminal domain of both the 43 kDa GyrB and 40 kDa MutL ATPase fragments (Wigley *et al*., 1991; Ban and Yang, 1998), and is an example of an unusual left-handed βαβ crossover seen in proteins such as EF-G, ribosomal protein S5 and RNase

Table I. Data collection, refinement and stereochemistry

Data collection	Native 1[a]	Se-met peak 1	Se-met remote 1	Se-met (native) 2[a]	Se-met peak 2	Se-met remote 2
Resolution (Å)	20 – 2.0	20 – 2.5	20 – 2.7	20 – 2.3	30 – 2.8	30 – 2.9
Wavelength (Å)	1.127	0.9793	1.078	1.100	0.9796	1.100
Space group	$P2_12_12$			$P2_12_12$		
I/σ (last shell)	16.7 (2.7)	13.1 (4.5)	13.3 (5.6)	10.0 (1.8)	16.2 (5.6)	16.7 (6.7)
R_{sym}[b] (last shell) (%)	0.058 (0.405)	0.075 (0.211)	0.073 (0.171)	0.111 (0.473)	0.085 (0.234)	0.079 (0.177)
Completeness (last shell) %	95.8 (90.6)	96.7 (94.9)	96.6 (93.8)	96.1 (88.9)	98.5 (87.3)	98.9 (93.4)
No. of reflections	284 447	243 169	191 859	2 006 747	2 043 065	1 861 489
Unique	37 738	19 710	15 640	149 698	84 924	76 768
No. of sites	–	5	5	–	30	30
Refinement	**Crystal form 1[a]**			**Crystal form 2[a]**		
Resolution (Å)	20 – 2.0			20 – 2.3		
No. of reflections	34 608			137 434		
Working	31 478			124 899		
Free (% total)	3130 (8.3)			12 535 (8.4)		
R_{work}[c] (last shell) (%)	21.4 (26.0)			21.4 (25.7)		
R_{free}[c] (last shell) (%)	23.9 (30.2)			26.3 (30.7)		
Structure and stereochemistry	**Crystal form 1**			**Crystal form 2**		
No. of atoms	3932			23 098		
Protein	3684			22 053		
Water	246			853		
Nucleotide	0			186		
Ions	2			6		
R.m.s.d. bond lengths (Å)	0.011			0.013		
R.m.s.d. bond angles (°)	1.313			1.423		

[a]Crystal form 1, unliganded monomer; crystal form 2, AMP-PNP-bound dimer.
[b]$R_{sym} = \Sigma\Sigma_j|I_j - \langle I\rangle|/\Sigma I_j$, where I_j is the intensity measurement for reflection j and $\langle I\rangle$ is the mean intensity for multiply recorded reflections.
[c]$R_{work,\ free} = \Sigma||F_{obs}| - |F_{calc}||/|F_{obs}|$, where the working and free R-factors are calculated using the working and free reflection sets, respectively. The free reflections were held aside throughout refinement.

P (Ramakrishnan and White, 1992; Ævarsson *et al*., 1994; Czworkowski *et al*., 1994; Murzin, 1995; Stams *et al*., 1998). In gyrase, this domain has been proposed to mediate intersubunit communication by structurally transducing signals from the ATP binding and hydrolysis site of the GHKL domain to the DNA binding and cleavage domains of the gyrase holoenzyme. The architecture of the topoVI-B′ 'transducer' domain is slightly more diverged from the equivalent region of GyrB than is the GHKL domain, but is still a very close structural match. The Cα r.m.s.d. for core secondary structural elements is 1.54 Å over 54 amino acids (Figure 2C), a structural similarity that is all the more remarkable given that <11% sequence identity exists between these two domains. The only point at which the structure of the transducer domain of topoVI-B′ differs significantly from that seen in GyrB is at its C-terminal-most α-helix. In GyrB, this helix bends back sharply towards a molecular two-fold axis to interact with a dimer-related helix, while in the topoVI-B′ monomer structure, this helix is straight. It does not appear that the sharp bend observed in the GyrB C-terminal helix could be accommodated by topoVI-B′. The GyrB C-terminal helix is anchored to the core of the transducer domain by a number of hydrophobic residues after the bend, whereas the topoVI-B′ helix becomes highly polar immediately upon its protrusion from the transducer domain core.

Nucleotide-bound structure

To understand the effects of ATP binding on topoVI-B, we co-crystallized topoVI-B′ with the non-hydrolyzable ATP analog AMP-PNP. These crystals belong to space group $P2_12_12$ and contain six protein chains per asymmetric unit. The AMP-PNP form was solved to 2.3 Å resolution using MAD with selenomethionine-labeled protein. The final model contains 97% of all residues in the six protein chains (see Materials and methods), and was refined to an R-factor of 21.4% and an R_{free} of 26.4%. The six protomers in the asymmetric unit superimpose closely, with a C_α r.m.s.d. of ~0.5 Å for any given pair.

The GHKL domains of type IIA topoisomerases and MutL proteins are known to dimerize in response to ATP binding. In the strand passage reaction of type IIA topoisomerases, this step represents the closure of the 'entry' or 'N-gate' of the enzyme (Osheroff, 1986; Roca and Wang, 1992; Ali *et al*., 1995). Strikingly, we observe that topoVI-B′ also dimerizes when bound to AMP-PNP, creating an interprotomer interaction that is very similar to that seen in the GyrB and MutL ATPase fragment structures (Figure 3; Wigley *et al*., 1991; Ban *et al*., 1999). This interaction is mediated almost entirely between the lateral sides of the GHKL domains of each monomer.

The topoVI-B′ dimerization interaction also shares a second prominent structural feature with the GyrB and MutL dimer structures, in which the first 10–15 N-terminal amino acids of one protomer extend outward and latch onto the top of the GHKL domain of the opposite protomer. Each of these N-terminal 'straps' buries ~570 Å^2 of surface area. Additionally, 1630 Å^2 of each GHKL domain, 530 Å^2 of each H2TH domain and 550 Å^2 of each transducer domain are buried upon dimerization.

Mutational analysis of the GyrB N-terminal strap has identified residues that are critical for dimerization, including a conserved isoleucine (Ile10 in GyrB; Brino *et al*., 1997, 1999, 2000), which binds in a hydrophobic pocket and anchors the strap to the opposite protomer (Wigley *et al*., 1991). In topoVI-B′, Phe7 appears to play an analogous role, binding in the same hydrophobic pocket as Ile10 of GyrB. Interestingly, another strap residue shown to be important in GyrB, Tyr5, appears to have no functional counterpart in topoVI-B′. It remains to be seen whether the absence of this tyrosine is important to function in topoVI-B′. The conservation of dimerization geometry and the N-terminal strap in topoVI-B′ further emphasizes its mechanistic similarity to type IIA topoisomerases.

The H2TH domains of topoVI-B′ also contribute to the dimer interface, packing against the GHKL domain of the dimer-related subunit. In the monomer form, this domain partially occludes the GHKL domain dimer interface, and it moves ~9 Å upon dimerization to open up this surface. The role of the H2TH domains in the mechanism of topoVI is unknown, and topoVI-B does not share any obvious activities with Fpg/endoVIII glycosylases other than as a general DNA-binding protein (Melamede *et al*., 1994). One may speculate that this domain could assist with binding of DNA to the enzyme or, given its proximity to the ATP-binding pockets, could affect nucleotide turnover.

In the structure of a nucleotide-bound dimer form of the 43 kDa GyrB ATPase fragment, the inner sides of the transducer domains, together with their kinked, C-terminal-most helices and the GHKL dimer interface, enclose a hole ~20 Å in diameter (Figure 3B; Wigley *et al*., 1991). This hole has been proposed to accommodate a captured T-segment prior to the strand passage reaction (Wigley *et al*., 1991; Tingey and Maxwell, 1996). In the topoVI-B′ dimer structure, the space between the transducer domains is only ~16 Å at its widest, and the C-terminal helices do not bend and cross over one another as seen in gyrase. As a result, there is no hole formed by the topoVI-B′ dimer that is analogous to that observed for the GyrB ATPase fragment. Because non-crystallographic symmetry in this crystal form affords three independent views of the topoVI-B′ dimer, and given that the polar character of its C-terminal transducer helices appears to preclude their bending back toward the two-fold axis of the dimer, it seems unlikely that the lack of the hole in topoVI-B′ is due to crystal packing artifacts. Rather, these features suggest that despite the overall architectural and catalytic similarity of topoVI-B′ to GyrB, the C-terminal end of topoVI-B has been adapted to interact with the altered DNA binding and cleavage machinery used by the topoVI-A subunit.

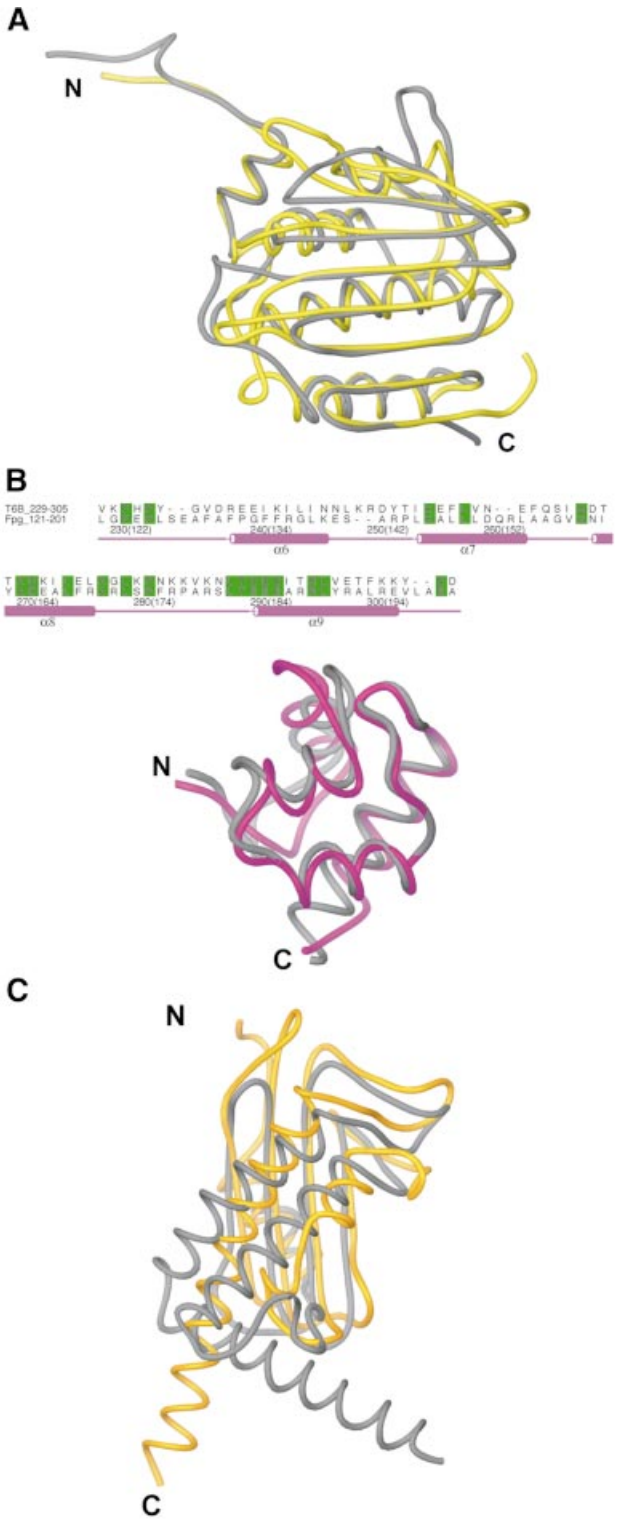

Fig. 2. Superposition of topoVI-B′ domains with GyrB and Fpg. (**A**) Least-squares superposition of the GHKL domains of topoVI-B′ (yellow) and *E.coli* gyrase B (gray) (Wigley *et al*., 1991). The N- and C-termini of the domains are labeled. (**B**) Top: structure-based sequence alignment of the H2TH domain of topoVI-B′ (residues 229–305) with the H2TH domain of *T.thermophilus* Fpg (residues 121–201; Sugahara *et al*., 2000). Conserved residues are highlighted in green. The domains share 24% sequence identity and 43% similarity over 77 residues. The residue numbering is that of topoVI-B′ followed by that of Fpg in parentheses. Bottom: least-squares superposition of the H2TH domains of topoVI-B′ (pink) and Fpg (gray). (**C**) Least-squares superposition of the transducer domains of topoVI-B′ (orange) and gyrase B (gray) (Wigley *et al*., 1991). The C-terminal helices of the two proteins, which have different configurations, were not used in the superposition.

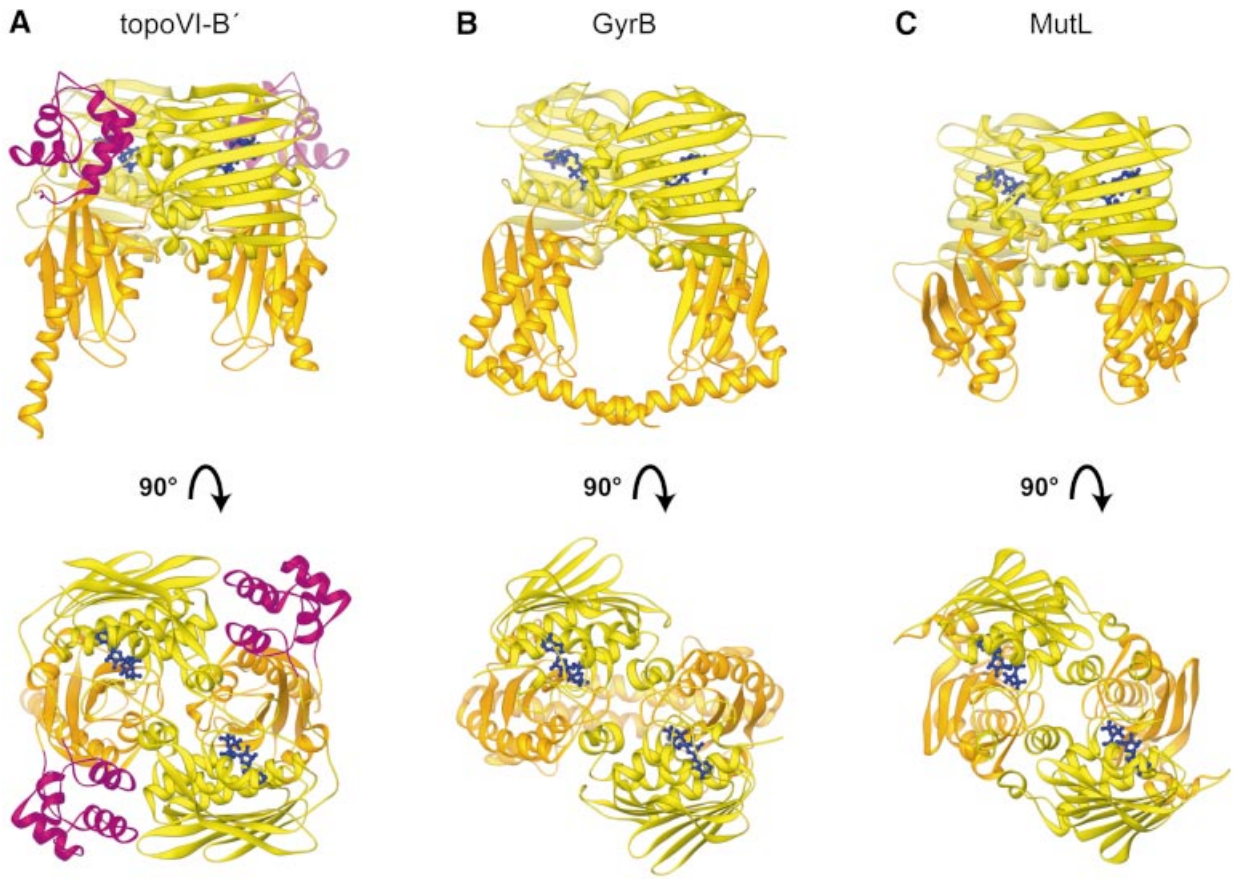

Fig. 3. Comparison of topoVI-B′, GyrB and MutL dimer structures. (**A**) Structure of the AMP-PNP bound topoVI-B′ dimer. Coloring is as in Figure 1C. Two views are shown: front (top) and top-down (bottom). Bound nucleotides and Mg^{2+} ions are shown in blue. (**B**) and (**C**) AMP-PNP-bound dimer structures of GyrB (Wigley *et al*., 1991) and MutL (Ban *et al*., 1999), respectively. The GHKL and transducer domains are colored as in (A), and the views are equivalent for all three proteins.

Intra- and interdomain rearrangements mediated by nucleotide binding

In addition to dimerization upon ATP binding, other structural changes are evident upon comparison of the AMP-PNP-bound and unbound topoVI-B′ structures. At the ATP-binding site, a number of side chain and main chain elements undergo local positional changes to become liganding groups for the bound nucleotide (Figure 4A). Asn42 binds a Mg^{2+} ion, which is also coordinated by the three phosphate groups of AMP-PNP and two water molecules; the two water molecules are in turn held in place by Glu38 and Glu41. Gly97 and Lys98, contained in a loop that is disordered in the unbound state, ligand the ribose and β-phosphate, respectively, while Asp76, Gly80 and Thr170 help position the adenine moiety. Finally, the glycine-rich P-loop (amino acids 107–111) moves by up to 6.4 Å from its position in the unbound state to form an extensive hydrogen bond network between four backbone amide nitrogens and the γ-phosphate of AMP-PNP (Figure 4A). Most of the residues involved in nucleotide contacts are part of the GHKL signature sequence motifs conserved in the type IIA topoisomerases and MutL proteins (Figure 1B), and are structurally analogous to nucleotide-binding residues in GyrB (Figure 4), illustrating the high degree of conservation in the nucleotide-binding pocket of the GHKL domains of these proteins.

The local structure of the transducer domain is also affected by nucleotide binding. The most dramatic difference in this region is that the loop immediately N-terminal to the C-terminal-most helix of this domain moves translationally by 5–6 Å, concomitantly flipping Lys427 by 180° and inserting it into the ATP-binding pocket of the GHKL domain (Figure 5A). This configurational change positions the Nζ of Lys427 within hydrogen bonding distance of a non-bridging oxygen of the γ-phosphate of AMP-PNP. Rearrangements of this loop region, together with a conserved lysine contacting an oxygen of the γ-phosphate, have also been observed in GyrB and MutL (Wigley *et al*., 1991; Ban and Yang, 1998; Ban *et al*., 1999; Lamour *et al*., 2002).

The motion of the loop containing Lys427 has significant structural consequences for the relative positioning of domains in topoVI-B′. Upon nucleotide binding and dimerization, the transducer domain rotates ~11° relative to its position in the apo structure, moving the distal end of the C-terminal helix by ~15 Å (Figure 5B). Each of the three copies of the dimer in the asymmetric unit displays an identical orientation of all three domains, indicating that these movements occur universally upon nucleotide

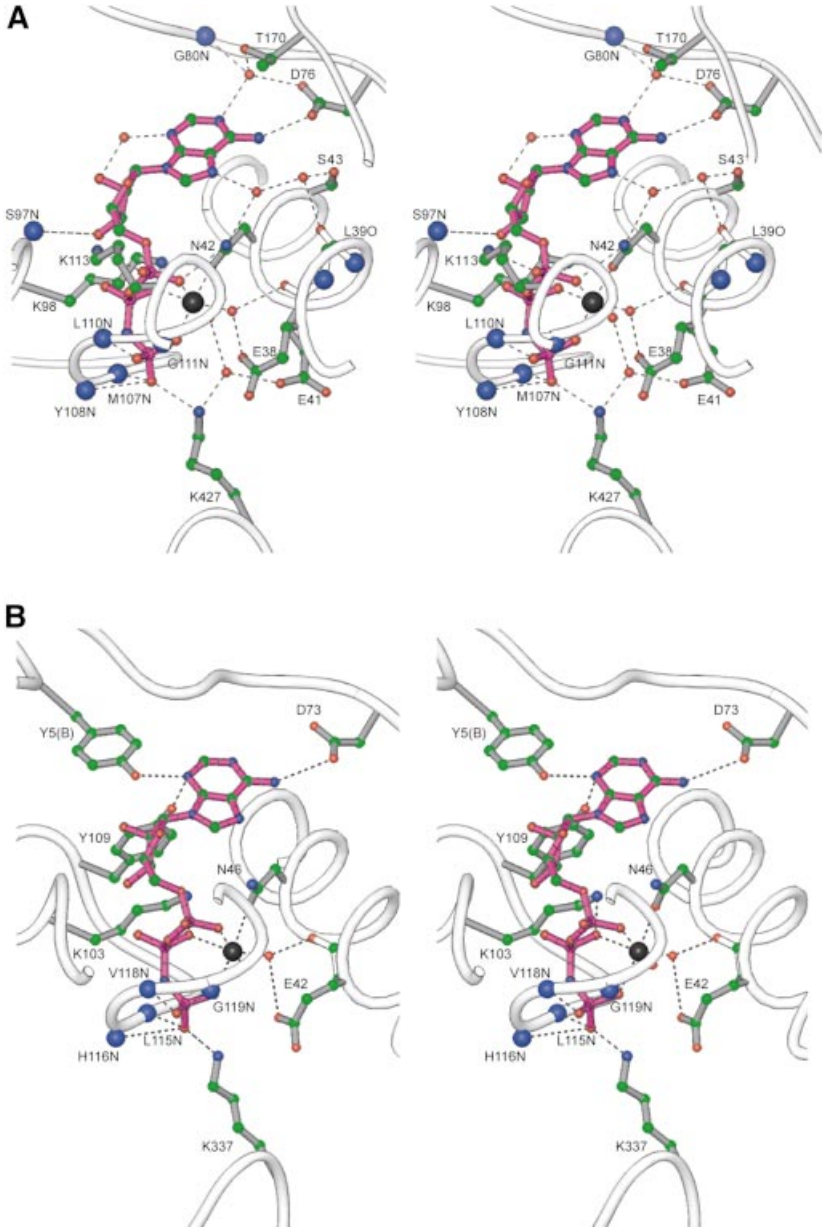

Fig. 4. Comparison of topoVI-B′ and GyrB ATP-binding sites. (**A**) Stereo view of AMP-PNP coordination by topoVI-B′. Bound AMP-PNP is shown in magenta, protein side chains in gray, and the protein backbone and specific main chain bonds in white. Hydrogen bonds are represented as dotted lines. Carbon atoms are shown in green, nitrogen in blue (main-chain nitrogen atoms enlarged for visualization), oxygen in red, phosphorus in pink and bound Mg^{2+} in black. Amino acids are labeled with their one-letter code and residue number. (**B**) Stereo view of AMP-PNP coordination by GyrB. The view and the color scheme are essentially identical to that in (A). Residue Y5(B) resides on the N-terminal strap of the opposite GyrB protomer and has no analog in topoVI-B′.

binding. Nucleotide binding has been shown to have similar structural effects on the orientation of GHKL and transducer domains in both GyrB and MutL, indicating that this motion may play a conserved role in the mechanisms of these proteins.

Discussion

The evolutionary relationship between type IIA and IIB topoisomerases

Prior to this study, interesting parallels, but also significant differences, had been observed between type IIA and IIB topoisomerases. The sequence and structure of the topoVI-A subunit revealed that the two families share the toprim and CAP domains important for DNA binding and cleavage (Aravind *et al*., 1998; Nichols *et al*., 1999). Biochemical data indicated that these domains play equivalent roles in both enzyme families (Bergerat *et al*., 1997; Nichols *et al*., 1999), even though the order and placement of the toprim and CAP modules are swapped between the two (Figure 1A). Nonetheless, the closest homolog to topoVI-A at the amino acid sequence level is not a type IIA DNA topoisomerase, but rather the meiotic recombination factor Spo11 (Bergerat *et al*., 1997; Keeney *et al*., 1997). These observations, together with sequence data indicating that the topoVI-B subunit shares GHKL

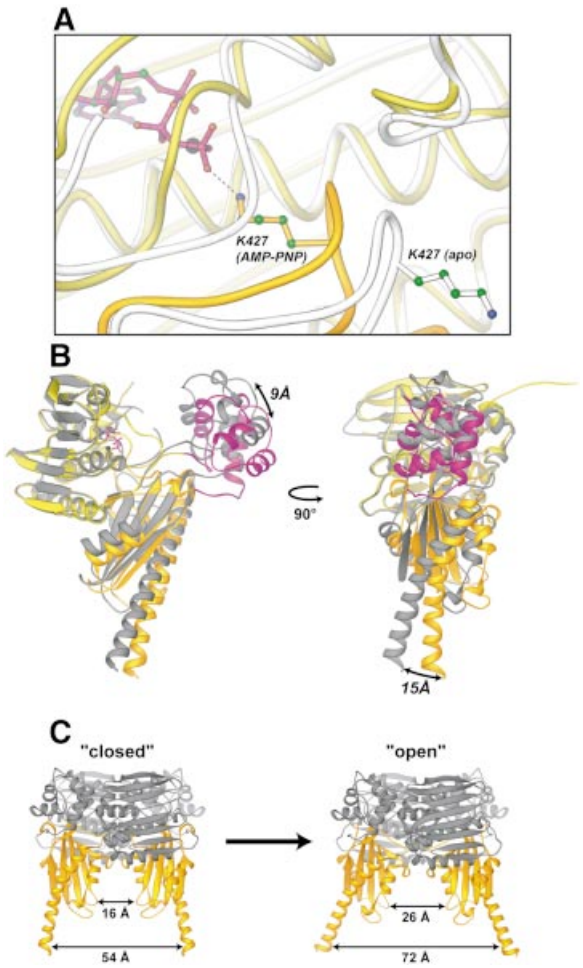

Fig. 5. Nucleotide binding induces structural changes in topoVI-B′. (**A**) Least-squares superposition of the topoVI-B′ ATP-binding site in both nucleotide states, highlighting γ-phosphate interactions. The apo form of the protein is colored white, while the AMP-PNP-bound form is colored as in Figure 1C, with the GHKL domain yellow and the transducer domain orange. The 'switch' lysine (K427) is observed to flip positions and hydrogen bond the γ-phosphate of bound AMP-PNP. (**B**) Superposition of topoVI-B′ monomers in both nucleotide-bound and unbound states. Only the GHKL domains were included for superposing the two states. Two views are shown, rotated 90° relative to each other. The apo form is colored gray and the AMP-PNP-bound form is colored as in Figure 1C. The 15 Å motion of the distal end of the C-terminal α-helix is depicted with an arrow (right panel), as is the 9 Å motion of the H2TH domain (left panel). (**C**) Model for topoVI-B′ transducer motions in a dimerized state. A 'closed' AMP-PNP-bound GHKL/transducer domain orientation (left) is shown next to a modeled 'open' configuration (right). The 'open' model was created by combining the GHKL/transducer domain orientations seen in the topoVI-B′ apo structure with the GHKL/H2TH dimer geometry of the AMP-PNP-bound structure. The space between transducer domains increases dramatically in this configuration; the distances shown are between Cα atoms of Glu366 (upper arrows) and Lys466 (lower arrows).

sequence motifs with type IIA topoisomerases, left the evolutionary relationship between these enzymes obscure.

Our three-dimensional structures of topoVI-B′, both alone and in complex with AMP-PNP, now help to resolve this issue. The first 220 residues of topoVI-B′ adopt a GHKL family ATPase fold, as anticipated. Additionally, of the 10 GHKL proteins whose structures are known, the closest structural match to this region of topoVI-B is the GHKL domain of a type IIA topoisomerase, DNA gyrase (GyrB). Moreover, our data unexpectedly reveal that the third domain of topoVI-B is structurally homologous to the C-terminal half of the 43 kDa GyrB ATPase fragment (Wigley *et al*., 1991). This C-terminal region is thought to be important for transducing structural signals from the ATP-binding GHKL domains to the more distal DNA binding and cleavage regions of the enzyme (Wigley *et al*., 1991; Lamour *et al*., 2002). Its existence alongside the GHKL domain in topoVI-B provides clear evidence that type IIA and IIB topoisomerases use the same nucleotide-dependent machinery to effect DNA opening and transport, and indicates that they originally descended from a common ancestor.

ATP-coupled conformational changes in type II topoisomerases

In the DNA strand passage reaction of type IIA topoisomerases, the GHKL domains have been proposed to act as an 'entry' gate for the DNA segment to be transported (T-segment) (Kirchhausen *et al*., 1985; Wigley *et al*., 1991; Roca and Wang, 1992). The GHKL domains dimerize in response to ATP binding and, upon capture of a T-segment, trap it within the interior of the topoisomerase. Structural changes following nucleotide binding subsequently propagate throughout the enzyme, resulting in breakage and opening of the G-segment, passage of the T-segment though the break and expulsion of the T-segment through a protein 'exit' gate (Roca and Wang, 1994; Roca *et al*., 1996).

Although the exact physical consequences of ATP binding and hydrolysis by the GHKL domains are still enigmatic, structural data for the 43 kDa GyrB ATPase fragment have provided important insights into the conformational changes that accompany these events in type IIA topoisomerases. The ATP-binding site of GyrB consists primarily of residues from the GHKL fold, but also includes a loop from the transducer domain that extends into the active site. This loop contains an invariant lysine (Lys337) that forms a hydrogen bond with the γ-phosphate of bound nucleotide (Wigley *et al*., 1991). A recent structure of a nucleotide-free *Thermus thermophilus* GyrB dimer revealed that both this loop and its lysine can move away from the GHKL active site in the absence of ATP, causing a significant (~18°) interdomain rotation within each protomer (Lamour *et al*., 2002). The lysine has been proposed to act both as a catalytic residue and as a switch that senses the nucleotide-binding state of the protein and helps direct motions between the GHKL and transducer domains, a hypothesis that has been supported by mutagenesis studies of *E.coli* gyrase and *Drosophila melanogaster* topoisomerase II (Hu *et al*., 1998; Smith and Maxwell, 1998). A similar active site architecture and set of domain motions have also been observed in the nucleotide-bound and unbound structures of the distantly related MutL DNA repair protein (Ban and Yang, 1998; Ban *et al*., 1999).

This nucleotide-responsive conformational switch can now be further explored in the context of our topoVI-B′ models. TopoVI-B′ contains both the GHKL and transducer domains seen in GyrB and MutL, and also possesses a loop within the tranducer domain that contains an invariant lysine residue and is situated near the ATP-binding site. Nucleotide binding to topoVI-B′ repositions this loop, flipping the 'switch' lysine (Lys427) into the

ATP-binding pocket and coordinately rotating the transducer domain ~11° relative to the GHKL domain. This large motion is amplified through the protruding C-terminal α-helix of the transducer domain to move the distal end of this helix ~15 Å (Figure 5), suggesting that this region may act as a 'lever arm' during the holoenzyme reaction (see below). The conservation of both overall structure and local nucleotide sensing elements argues that the nucleotide-dependent motions observed in GyrB, MutL, and now topoVI-B′, in fact represent a conserved mechanism within these enzyme families for structurally communicating the nucleotide-binding state of the GHKL domains to other regions of the enzyme.

The topoVI holoenzyme and a mechanism for strand passage

Type IIB topoisomerases have been discovered relatively recently compared with their eukaryotic and prokaryotic type IIA cousins, and, as a result, have been less thoroughly characterized. A physical framework for considering the DNA transport reaction of type IIB topoisomerases has derived primarily from biochemical data on *S.shibatae* topoVI from Forterre and co-workers (Bergerat *et al*., 1994, 1997; Buhler *et al*., 1998, 2001) and on the structure of the *M.jannaschii* topoVI-A subunit (Nichols *et al*., 1999). Enzymological characterization of topoVI indicates that the protein functions as a heterotetramer capable of passing one DNA duplex through another in an ATP-dependent manner (Bergerat *et al*., 1994, 1997). In the proposed mechanism for this reaction, ATP binding by the B subunit stimulates DNA cleavage by a bipartite CAP/toprim active site in the A subunit (Bergerat *et al*., 1997; Aravind *et al*., 1998; Nichols *et al*., 1999). The primary DNA binding and cleavage site appears to be a long, deep channel that is formed by dimerization of the A subunits; residues important for DNA cleavage in topoVI, and its ortholog Spo11, are positioned along the walls of this channel (Aravind *et al*., 1998; Nichols *et al*., 1999; Diaz *et al*., 2002). This structural arrangement suggests that the A subunit dimer separates during G-segment opening, and that the B subunits act as bridging elements to span the broken G-segment and prevent dsDNA break formation. Such a model invokes a simple 'two-gate' mechanism for the action of type IIB topoisomerases, whereby transported DNA enters through a nucleotide-dependent 'entry' gate comprised of the two B subunits, and leaves through an 'exit' gate on the opposite side of the protein, formed by the two A subunits. A lack of structural data for the B subunits, however, has left unclear the mechanism by which ATP binding and hydrolysis regulates the structural changes in the A subunits that open the exit gate.

The structures of unliganded and AMP-PNP-bound forms of topoVI-B′ help validate this mechanism for type IIB topoisomerases (Figure 6). In the assembly of the topoVI holoenzyme, the B subunits bind the A subunits in a 2:2 arrangement (Bergerat *et al*., 1994). Pull-down assays using full-length and truncated proteins indicate that the C-terminus of topoVI-B and the N-terminus of topoVI-A are involved in these interactions and may constitute part of the B/A oligomerization interface (K.D.Corbett and J.M.Berger, unpublished data). Our structural data further show that ATP binding to topoVI-B′ leads to dimerization of the subunits. Given that the topoVI holoenzyme also retains an A subunit dimerization interface, the holoenzyme assembly is limited to an architecture in which the ATP-binding B subunits project upward from the DNA binding and cleaving A subunits (Figure 6A). This organization leaves the B subunits free to act as an ATP-actuated T-segment entry gate, and in position to bridge the broken G-segment ends during strand passage, as predicted by a two-gate reaction mechanism (Figure 6B). In this scenario, the T-segment is temporarily trapped in a hole bound by the B subunits above and the A subunits below. This arrangement also provides an explanation for the dramatic increase in DNA cleavage seen upon ATP binding (Buhler *et al*., 2001); ATP-driven closure of the B subunits could directly alter the A subunit active site architecture through direct linkages between the C-termini of the topoVI-B transducer regions and the tyrosine-bearing CAP domains of topoVI-A (Buhler *et al*., 1998, 2001). It is tempting to speculate that the topoVI-A ortholog Spo11 may have a partner protein analogous to topoVI-B for repositioning active site residues to initiate DNA cleavage during meiotic recombination (Buhler *et al*., 2001).

The intrasubunit conformational changes we observe in topoVI-B′ upon nucleotide binding also indicate how the B subunits might direct G-segment opening. A comparison of the apo and AMP-PNP-bound topoVI-B′ structures shows that a distinct rotation between the GHKL and transducer domains occurs upon nucleotide binding (Figure 5B). Were this structural transition to reverse at some point after the GHKL domains had dimerized, the space between transducer domains would widen significantly (Figure 5C). This widening could, in turn, directly promote A subunit separation and subsequent T-segment release (Figure 6B). Curiously, inspection of the AMP-PNP-bound dimer of topoVI-B′ indicates that there is not enough space between the transducer domains to accommodate a double-stranded DNA segment. This suggests that strain induced by T-segment capture could help promote an open GHKL/transducer conformation, aiding A subunit separation (Corbett *et al*., 1992).

The idea that interdomain motions in topoVI-B direct G-segment opening and T-segment passage in type IIB enzymes, while based principally on structural and biochemical data on topoVI, is also consistent with data obtained for type IIA topoisomerases. For example, kinetic profiling experiments on *Saccharomyces cerevisiae* topoisomerase II have shown that one ATP is hydrolyzed by the enzyme before strand passage, while the second is hydrolyzed afterwards (Harkins *et al*., 1998; Baird *et al*., 1999). Based on these observations, Lindsley and coworkers proposed that the first ATP hydrolysis event in topoisomerase II invokes a conformational signal to catalyze strand passage: this signal was suggested to arise from conformational changes between the GHKL and transducer domains. Subsequent pre-steady-state studies of *S.cerevisiae* topoisomerase II further showed that the rate-limiting step of the strand passage reaction is the release of phosphate following the first ATP hydrolysis, and that this release is possibly preceded by a conformational change (Harkins *et al*., 1998; Baird *et al*., 2001). In topoVI-B′, ATP is completely enveloped by the GHKL and transducer domains upon binding, such that

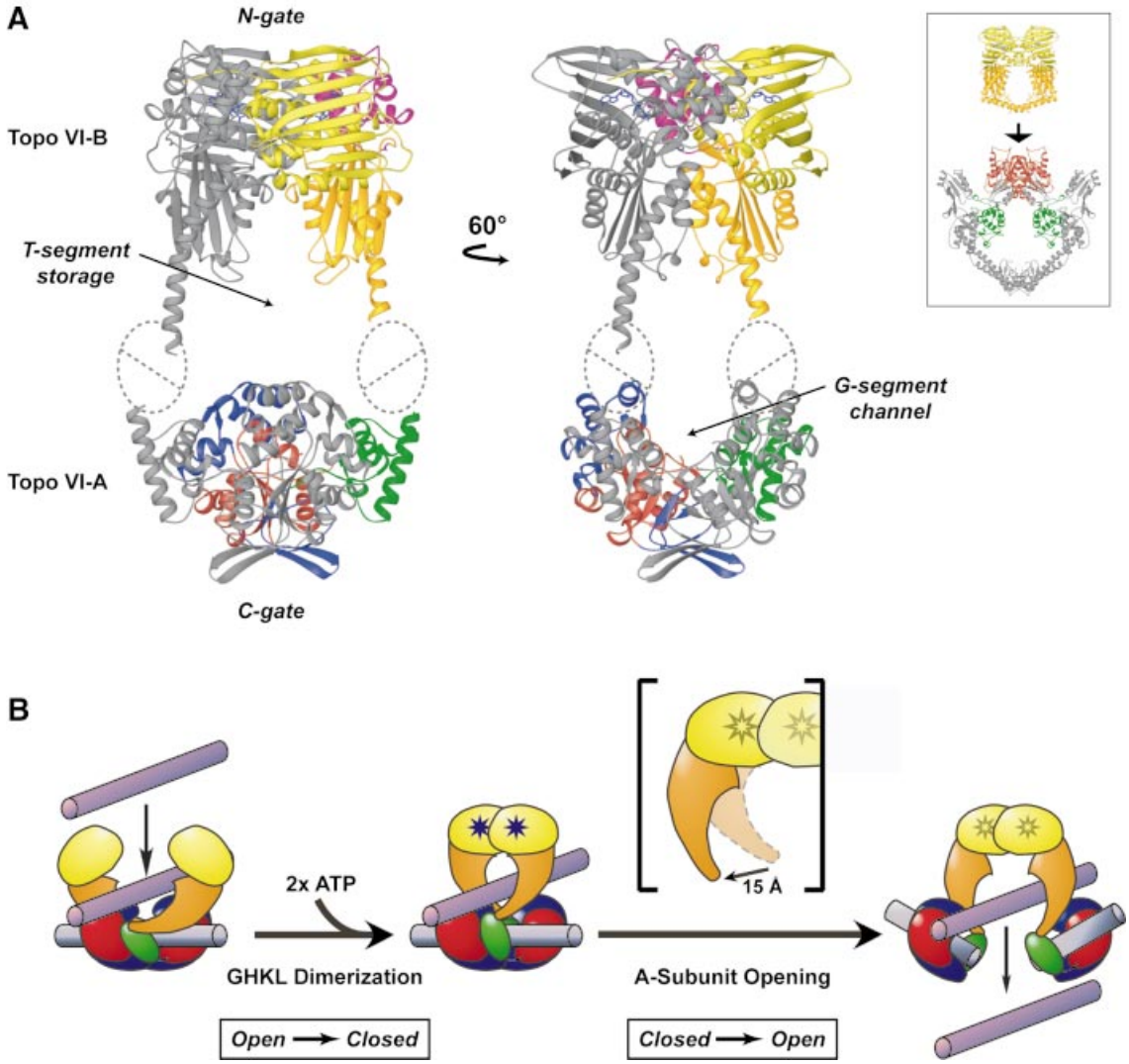

Fig. 6. The topoVI holoenzyme and strand passage reaction. (**A**) Model for the three-dimensional organization of the topoVI holoenzyme (B_2A_2 heterotetramer). The configuration is based on the AMP-PNP-bound topoVI-B′ structure, the *M.jannaschii* topoVI-A structure (Nichols *et al*., 1999) and the approximate locations of the interaction domains on each subunit, which consist of residues removed for crystallographic studies (residues 1–68 of topoVI-A, residues 471–529 of topoVI-B). One topoVI-A protomer is colored gray and the other is colored with the CAP domain green, the toprim domain red, and surrounding scaffold blue. One topoVI-B′ protomer is colored gray, the other is colored as in Figure 1C. The left panel shows the channel in the A subunit dimer that is proposed to bind the G-segment. Inset: a view of the probable organization of the type IIA topoisomerase holoenzyme, built from the structures of the GyrB ATPase fragment (top) (Wigley *et al*., 1991) and the DNA binding/cleavage domains of *S.cerevisiae* topoII (bottom) (Berger *et al*., 1996). Note that type IIA topoisomerases appear to have two cavities for T-segment storage during strand passage (one in the B subunit dimer and the other in the A subunit dimer), while type IIB enzymes appear to have only one. Domains are colored as in Figure 1A. (**B**) Proposed mechanism for strand passage by topoVI. Domains of the holoenzyme are colored as in (A). GHKL/transducer domain rearrangements (open→closed and closed→open) are shown in boxes. Left: a topoVI-A dimer binds a G-segment (gray), then a T-segment enters between the B subunits. Middle: dimerization of the topoVI-B GHKL domains upon binding ATP (blue stars) is the key event that traps the T-segment inside the enzyme. Right: subsequent ATP hydrolysis and/or phosphate release allows a conformational change in the B subunits leading to disruption of the A subunit dimer interface and release of the T-segment. While the A subunit dimer is disrupted, the B subunit dimer acts as an 'enzyme bridge' to hold the broken G-segment ends. The stars representing bound nucleotide in the final state are shaded gray to indicate that the nucleotide state of the enzyme in this state is unknown. Inset: One topoVI-B subunit is shown in schematic transitioning from the closed→open GHKL/transducer domain configuration as per Figure 5C.

inorganic phosphate freed by hydrolysis would remain trapped inside the active site until a conformational change allowed its release. A conformational switch from the 'closed' domain arrangement observed in our AMP-PNP structure to the 'open' state seen in our apo model could accommodate such an exit from the active site, perhaps through the space vacated by the switch lysine. Such consistency between mechanistic and structural data for the type IIA and IIB topoisomerases emphasizes further the relatedness of these enzyme families, and underscores the utility of comparative studies.

With the apo and AMP-PNP-bound structures of the topoisomerase VI-B subunit presented here, the structures of all major catalytic domains of the type IIB topoisomerase family have now been determined. Our data show that while topoVI has some properties distinct from type IIA topoisomerases, it is certainly an evolutionary cousin to its eukaryotic and bacterial counterparts. It is especially

noteworthy that the energy-transducing and DNA-cleavage mechanisms of these molecular machines have been conserved, even though their overall DNA binding and transport architectures have been dramatically rearranged. These catalytic similarities allow us to use structural data from topoVI-B′ to better understand the mechanism by which both families of type II topoisomerases use ATP binding and hydrolysis to effect large-scale allosteric changes and transport one DNA duplex through another. Moreover, since many of the catalytic modules found in type IIB topoisomerases can also be found in a number of other cellular processes, from DNA repair (MutL) to meiotic recombination (Spo11), future work toward understanding topoVI should provide useful insights for understanding the mechanisms of these diverse biophysical systems as well.

Materials and methods

Protein purification

The *top6b* gene was amplified by PCR from *S.shibatae* genomic DNA prepared from a Qiagen genomic DNA Prep Kit. The resulting PCR product was cloned into a derivative of pET24b coding for an N-terminal tobacco etch virus (TEV) protease-cleavable His_6 tag. Protein was overexpressed in *E.coli* cells containing a plasmid coding for the expression of several rare tRNA codons [BL21-CodonPlus(DE3)-RIL, Stratagene; Kane, 1995]. Cells were induced with 0.5 mM isopropyl-β-D-thiogalactopyranoside (IPTG) at A_{600} = 0.3 and grown for 4 h at 37°C. Cells were then harvested by centrifugation and resuspended in buffer A [20 mM HEPES pH 7.5, 10% glycerol, 2 mM β-mercaptoethanol (β-ME)] plus 800 mM NaCl, 10 mM imidazole, 50 μg/ml lysozyme and protease inhibitors [0.1 mM phenylmethylsulfonyl fluoride (PMSF), 1 μg/ml leupeptin, 1 μg/ml pepstatin], and frozen dropwise into liquid nitrogen. Purification of topoVI-B was as follows: cells were thawed, sonicated and centrifuged. The clarified lysate was placed at 65°C for 15 min, on ice for 15 min and recentrifuged. The supernatant was passed through a 10 ml Ni-NTA Superflow (Qiagen) column; the column was washed with resuspension buffer, then washed again with buffer A plus 200 mM NaCl, 10 mM imidazole and protease inhibitors. The protein was eluted directly onto a 5 ml HiTrap heparin column (Amersham Pharmacia Biotech) with 250 mM imidazole, then eluted using a 200–550 mM NaCl gradient. Peak fractions were determined by SDS–PAGE, pooled and concentrated to ~2 ml by ultrafiltration (Amicon, Centriprep-10), and incubated overnight at 4°C with His_6-tagged TEV protease (Kapust and Waugh, 1999) using a w/w ratio of 1:30 TEV protease:topoVI-B. This mixture was diluted with buffer A plus 200 mM NaCl to a final imidazole concentration of 15 mM and subsequently passed through Ni-NTA resin again to remove the cleaved His_6 tag, uncleaved protein and TEV protease. Flow-through was concentrated to 2 ml and passed over an S-200 gel filtration column (Amersham Pharmacia Biotech). Peak fractions were concentrated to ~15 mg/ml as measured by absorbance at 280 nm in guanidine hydrochloride (Edelhoch, 1967). Purity was judged to be >98% by Coomassie Blue-stained SDS–PAGE. A contaminant in the full-length protein preparations was identified as a C-terminal proteolytic cleavage product of topoVI-B at residue 470 by mass spectrometry.

The coding sequence including residues 2–470 of *top6B* (topoVI-B′) was amplified by PCR and cloned as full-length *top6b*. Expression and purification of the protein were identical to that of the full-length protein, except that the heparin column step was not performed. Selenomethionine-containing protein was prepared as described previously (Van Duyne *et al*., 1993). Purification of selenomethionine-labeled protein was performed as for native proteins, with the addition of 5 mM β-ME in the initial steps, and the addition of 1 mM Tris(2-carboxyethyl)phosphine (TCEP) (Fluka) in the gel-filtration step and thereafter.

Crystallization and structure determination

For crystallization trials, purified topoVI-B′ was dialyzed overnight against 20 mM Tris–HCl pH 7.0 and 100 mM NaCl (plus 1 mM TCEP for selenomethionine protein), and the protein concentration was adjusted to 12 mg/ml. TopoVI-B′ was crystallized in microbatch format under paraffin oil (Hampton Research). For crystal form 1 (no nucleotide), protein solution was mixed 1:1 with well solution containing 20% PEG-3000, 100 mM Tris–HCl pH 7.0 and 200 mM $Ca(OAc)_2$. Crystals (rhomboidal plates, ~50 × 50 × 5 μm) grew within 24 h at 20°C. Crystals were transferred to cryoprotectant solution containing 10% PEG-3000, 50 mM Tris–HCl pH 7.0, 100 mM $Ca(OAc)_2$ and 25% glycerol for 1 min, then looped from the drop and flash-frozen in liquid nitrogen. The crystals were in space group $P2_12_12$, with unit cell dimensions a = 94.091 Å, b = 110.968 Å, c = 54.544 Å, α = β = γ = 90.0°.

For crystal form 2 (complexed to AMP-PNP), protein solution was mixed 1:1 with well solution containing 20% PEG-3000, 100 mM sodium citrate pH 5.5, 1 mM AMP-PNP (Sigma) and 10 mM $MgCl_2$ under paraffin oil. Crystals (thick blades) appeared in 12–24 h and grew to a maximum size of ~400 × 50 × 50 μm in 2 weeks. Crystals were transferred to cryoprotectant solution containing 10% PEG-3000, 50 mM sodium citrate and 25% PEG-400 for 1 min, then looped from the drop and flash-frozen in liquid nitrogen. The crystals were in space group $P2_12_12$ with unit cell dimensions a = 146.564 Å, b = 218.682 Å, c = 106.751 Å, α = β = γ = 90.0°.

All datasets were collected on Beamline 8.3.1 at the Advanced Light Source at Lawrence Berkeley National Laboratory. Data for all crystals were indexed and reduced with DENZO/SCALEPACK (Otwinowski and Minor, 1997), except for the high-resolution dataset of crystal form 2, which was indexed, reduced and scaled by the ELVES crystallography software package (J.M.Holton and T.Alber, unpublished results). The CCP4 set of programs was used for truncating and scaling the remaining data sets (CCP4, 1994). Phase calculation and density modification were carried out with SHARP and SOLOMON, respectively (Abrahams and Leslie, 1996; de La Fortelle and Bricogne, 1997). Model building was performed with O (Jones *et al*., 1991). In crystal form 1, residues 10–96 and 98–470 of topoVI-B′ were traceable into the original density-modified maps; the final structure comprised amino acids 10–96 and 98–470 of the native topoVI-B sequence, with amino acids 95, 96 and 98 modeled as alanine. A total of 91.3% (366) of non-glycine residues were in the most favored regions of Ramachandran space, with 8.5% (34) in additionally allowed regions, one residue in a generously allowed region and none in disallowed regions. In crystal form II, each of the six monomers was built individually. Initial refinement stages included non-crystallographic symmetry and phase restraints. Most regions of each protomer were visible, but some surface loops of some chains remained disordered even after refinement. The final model contained residues 4–467 of chain A (164–166 not modeled, 463–467 modeled as Ala), 4–458 of chain B (164–165 modeled as Ala), 4–469 of chain C (165 modeled as Ala), 4–464 of chain D (165 modeled as Ala), 4–461 of chain E (165–166 not modeled) and 4–463 of chain F (165–167 and 403 not modeled, 135–138, 161–164, 250, 362, 366, 398–399, 406–407, 455 and 458 modeled as Ala). The R-factor and R_{free} values of the final model were 21.4 and 26.3%, respectively. A total of 88.3% (2121) of non-glycine residues were in the most favored regions of Ramachandran space, with 11.6% (278) in additionally allowed regions, 0.2% (4) in generously allowed regions and none in disallowed regions. Refinement for all models was carried out using a Refmac/ARP procedure (Lamzin and Wilson, 1993; Murshudov *et al*., 1997), followed by TLS refinement as implemented in Refmac5 (Winn *et al*., 2001).

Coordinates

The coordinates have been deposited in the RCSB Protein Data Bank under accession Nos 1MU5 (crystal form 1) and 1MX0 (crystal form 2).

Acknowledgements

The authors would like to thank E.Skordalakes for assistance with data collection and processing, J.M.Holton for assistance at ALS beamline 8.3.1 and for the use of the ELVES software package, D.King for mass spectrometry analysis, D.Waugh for a plasmid coding for His_6-tagged TEV protease, N.Pokala and T.Handel for the modified pET24b expression vector, and J.E.Lindsley, D.S.Classen and J.P.Erzberger for critical reading of and comments on the manuscript. K.D.C. is a National Science Foundation Graduate Fellow and J.M.B. acknowledges support from the NCI (CA77373).

References

Abrahams,J.P. and Leslie,A.G.W. (1996) Methods used in the structure determination of bovine mitochondrial F_1 ATPase. *Acta Crystallogr. D*, **52**, 30–42.

Ævarsson,A., Brazhnikov,E., Garber,M., Zheltonosova,J., Chirgadze,Y., al-Karadaghi,S., Svensson,L.A. and Liljas,A. (1994) Three-dimensional structure of the ribosomal translocase: elongation factor G from *Thermus thermophilus*. *EMBO J.*, **13**, 3669–3677.

Ali,J.A., Orphanides,G. and Maxwell,A. (1995) Nucleotide binding to the 43-kilodalton N-terminal fragment of the DNA gyrase B protein. *Biochemistry*, **34**, 9801–9808.

Aravind,L., Leipe,D.D. and Koonin,E.V. (1998) Toprim: a conserved catalytic domain in type IA and II topoisomerases, DnaG-type primases, OLD family nucleases and RecR proteins. *Nucleic Acids Res.*, **26**, 4205–4213.

Baird,C.L., Harkins,T.T., Morris,S.K. and Lindsley,J.E. (1999) Topoisomerase II drives DNA transport by hydrolyzing one ATP. *Proc. Natl Acad. Sci. USA*, **96**, 13685–13690.

Baird,C.L., Gordon,M.S., Andrenyak,D.M., Marecek,J.F. and Lindsley,J.E. (2001) The ATPase reaction cycle of yeast DNA topoisomerase II. Slow rates of ATP resynthesis and P_i release. *J. Biol. Chem.*, **276**, 27893–27898.

Ban,C. and Yang,W. (1998) Crystal structure and ATPase activity of MutL: implications for DNA repair and mutagenesis. *Cell*, **95**, 541–552.

Ban,C., Junop,M. and Yang,W. (1999) Transformation of MutL by ATP binding and hydrolysis: a switch in DNA mismatch repair. *Cell*, **97**, 85–97.

Barton,G.J. (1993) ALSCRIPT: a tool to format multiple sequence alignments. *Protein Eng.*, **6**, 37–40.

Berger,J.M., Gamblin,S.J., Harrison,S.C. and Wang,J.C. (1996) Structure and mechanism of DNA topoisomerase II. *Nature*, **379**, 225–232.

Bergerat,A., Gadelle,D. and Forterre,P. (1994) Purification of a DNA topoisomerase II from the hyperthermophilic archaeon *Sulfolobus shibatae*: a thermostable enzyme with both bacterial and eucaryal features. *J. Biol. Chem.*, **269**, 27663–27669.

Bergerat,A., De Massy,B., Gadelle,D., Varoutas,P.-C., Nicolas,A. and Forterre,P. (1997) An atypical topoisomerase II from archaea with implications for meiotic recombination. *Nature*, **386**, 414–417.

Brino,L., Mousli,M., Oudet,P. and Weiss,E. (1997) Expression in *Escherichia coli* of Y5-mutant and N-terminal domain-deleted DNA gyrase B proteins affects strongly plasmid maintenance. *Plasmid*, **38**, 188–201.

Brino,L., Bronner,C., Oudet,P. and Mousli,M. (1999) Isoleucine 10 is essential for DNA gyrase B function in *Escherichia coli*. *Biochimie*, **81**, 973–980.

Brino,L., Urzhumtsev,A., Mousli,M., Bronner,C., Mitschler,A., Oudet,P. and Moras,D. (2000) Dimerization of *Escherichia coli* DNA-gyrase B provides a structural mechanism for activating the ATPase catalytic center. *J. Biol. Chem.*, **275**, 9468–9475.

Buhler,C., Gadelle,D., Forterre,P., Wang,J.C. and Bergerat,A. (1998) Reconstitution of DNA topoisomerase VI of the thermophilic archaeon *Sulfolobus shibatae* from subunits separately overexpressed in *Escherichia coli*. *Nucleic Acids Res.*, **26**, 5157–5162.

Buhler,C., Lebbink,J.H.G., Bocs,C., Ladenstein,R. and Forterre,P. (2001) DNA topoisomerase VI generates ATP-dependent double-strand breaks with two-nucleotide overhangs. *J. Biol. Chem.*, **276**, 37215–37222.

Carson,M. (1991) Ribbons 2.0. *J. Appl. Crystallogr.*, **24**, 958–961.

Celerin,M., Merino,S.T., Stone,J.E., Menzie,A.M. and Zolan,M.E. (2000) Multiple roles of Spo11 in meiotic chromosome behavior. *EMBO J.*, **19**, 2739–2750.

Champoux,J.J. (2001) DNA topoisomerases: structure, function and mechanism. *Annu. Rev. Biochem.*, **70**, 369–413.

CCP4 (1994) The CCP4 Suite: programs for protein crystallography. *Acta Crystallogr. D*, **50**, 760–763.

Corbett,A.H., Zechiedrich,E.L. and Osheroff,N. (1992) A role for the passage helix in the DNA cleavage reaction of eukaryotic topoisomerase II. A two-site model for enzyme-mediated DNA cleavage. *J. Biol. Chem.*, **267**, 683–686.

Czworkowski,J., Wang,J., Steitz,T.A. and Moore,P.B. (1994) The crystal structure of elongation factor G complexed with GDP, at 2.7 Å resolution. *EMBO J.*, **13**, 3661–3668.

de La Fortelle,E. and Bricogne,G. (1997) Maximum-likelihood heavy-atom parameter refinement for multiple isomorphous replacement and multiwavelength anomalous diffraction methods. *Methods Enzymol.*, **276**, 472–494.

Diaz,R.L., Alcid,A.D., Berger,J.M. and Keeney,S. (2002) Identification of residues in yeast Spo11p critical for meiotic DNA double-strand break formation. *Mol. Cell. Biol.*, **22**, 1106–1115.

Dutta,R. and Inouye,M. (2000) GHKL, an emergent ATPase/kinase superfamily. *Trends Biochem. Sci.*, **25**, 24–28.

Edelhoch,H. (1967) Spectroscopic determination of tryptophan and tyrosine in proteins. *Biochemistry*, **6**, 1948–1954.

Fromme,J.C. and Verdine,G.L. (2002) Structural insights into lesion recognition and repair by the bacterial 8-oxoguanine DNA glycosylase MutM. *Nat. Struct. Biol.*, **9**, 544–552.

Gilboa,R., Zharkov,D.O., Golan,G., Fernandes,A.S., Gerchman,S.E., Matz,E., Kycia,J.H., Grollman,A.P. and Shoham,G. (2002) Structure of formamidopyrimidine-DNA glycosylase covalently complexed to DNA. *J. Biol. Chem.*, **277**, 19811–19816.

Harkins,T.T., Lewis,T.J. and Lindsley,J.E. (1998) Pre-steady-state analysis of ATP hydrolysis by *Saccharomyces cerevisiae* DNA topoisomerase II. 2. Kinetic mechanism for the sequential hydrolysis of two ATP. *Biochemistry*, **37**, 7299–7312.

Hartung,F. and Puchta,H. (2001) Molecular characterization of homologues of both subunits A (SPO11) and B of the archaebacterial topoisomerase 6 in plants. *Gene*, **271**, 81–86.

Hartung,F., Angelis,K.J., Meister,A., Schubert,I., Melzer,M. and Puchta,H. (2002) An archaebacterial topoisomerase homolog not present in other eukaryotes is indispensable for cell proliferation of plants. *Curr. Biol.*, **12**, 1787–1791.

Hu,T., Chang,S. and Hsieh,T. (1998) Identifying Lys359 as a critical residue for the ATP-dependent reactions of *Drosophila* DNA topoisomerase II. *J. Biol. Chem.*, **273**, 9586–9592.

Jones,T.A., Zou,J.Y., Cowan,S.W. and Kjeldgaard,M. (1991) Improved methods for building protein models in electron density maps and the location of errors in these models. *Acta Crystallogr. A*, **47**, 110–119.

Kane,J.F. (1995) Effects of rare codon clusters on high-level expression of heterologous proteins in *Escherichia coli*. *Curr. Opin. Biotechnol.*, **6**, 494–500.

Kapust,R.B. and Waugh,D.S. (1999) *Escherichia coli* maltose-binding protein is uncommonly effective at promoting the solubility of polypeptides to which it is fused. *Protein Sci.*, **8**, 1668–1674.

Keeney,S., Giroux,C.N. and Kleckner,N. (1997) Meiosis-specific DNA double-strand breaks are catalyzed by Spo11, a member of a widely conserved protein family. *Cell*, **88**, 375–384.

Kirchhausen,T., Wang,J.C. and Harrison,S.C. (1985) DNA gyrase and its complexes with DNA: direct observation by electron microscopy. *Cell*, **41**, 933–943.

Lamour,V., Hoermann,L., Jeltsch,J.-M., Oudet,P. and Moras,D. (2002) An open conformation of the *Thermus thermophilus* gyrase B ATP-binding domain. *J. Biol. Chem.*, **277**, 18947–18953.

Lamzin,V.S. and Wilson,K.S. (1993) Automated refinement of protein models. *Acta Crystallogr. D*, **49**, 129–147.

Martini,E. and Keeney,S. (2002) Sex and the single (double-strand) break. *Mol. Cell*, **9**, 700–702.

Melamede,R.J., Hatahet,Z., Kow,Y.W., Ide,H. and Wallace,S.S. (1994) Isolation and characterization of endonuclease VIII from *Escherichia coli*. *Biochemistry*, **33**, 1255–1264.

Murshudov,G.N., Vagin,A.A. and Dodson,E.J. (1997) Refinement of macromolecular structures by the maximum-likelihood method. *Acta Crystallogr. D*, **53**, 240–255.

Murzin,A.G. (1995) A ribosomal protein module in EF-G and DNA gyrase. *Nat. Struct. Biol.*, **2**, 25–26.

Nichols,M.D., DeAngelis,K., Keck,J.L. and Berger,J.M. (1999) Structure and function of an archaeal topoisomerase VI subunit with homology to the meiotic recombination factor Spo11. *EMBO J.*, **18**, 6177–6188.

Osheroff,N. (1986) Eukaryotic topoisomerase II. Characterization of enzyme turnover. *J. Biol. Chem.*, **261**, 9944–9950.

Otwinowski,Z. and Minor,W. (1997) Processing of X-ray diffraction data collected in oscillation mode. *Methods Enzymol.*, **276**, 472–494.

Ramakrishnan,V. and White,S.W. (1992) The structure of ribosomal protein S5 reveals sites of interaction with 16S rRNA. *Nature*, **358**, 768–771.

Roca,J. and Wang,J.C. (1992) The capture of a DNA double helix by an ATP-dependent protein clamp: a key step in DNA transport by type II DNA topoisomerases. *Cell*, **71**, 833–840.

Roca,J. and Wang,J.C. (1994) DNA transport by a type II DNA topoisomerase: evidence in favor of a two-gate mechanism. *Cell*, **77**, 609–616.

Roca,J., Berger,J.M., Harrison,S.C. and Wang,J.C. (1996) DNA transport by a type II topoisomerase: direct evidence for a two-gate mechanism. *Proc. Natl Acad. Sci. USA*, **93**, 4057–4062.

Serre,L., Pereira De Jesus,K., Boiteux,S., Zelwer,C. and Castaing,B. (2002) Crystal structure of the *Lactococcus lactis*

formamidopyrimidine-DNA glycosylase bound to an abasic site analogue-containing DNA. *EMBO J.*, **21**, 2854–2865.
Smith,C.V. and Maxwell,A. (1998) Identification of a residue involved in transition-state stabilization in the ATPase reaction of DNA gyrase. *Biochemistry*, **37**, 9658–9667.
Stams,T., Niranjanakumari,S., Fierke,C.A. and Christianson,D.W. (1998) Ribonuclease P protein structure: evolutionary origins in the translational apparatus. *Science*, **280**, 752–755.
Sugahara,M., Mikawa,T., Kumasaka,T., Yamamoto,M., Kato,R., Fukuyama,K., Inoue,Y. and Kuramitsu,S. (2000) Crystal structure of a repair enzyme of oxidatively damaged DNA, MutM (Fpg), from an extreme thermophile, *Thermus thermophilus* HB8. *EMBO J.*, **19**, 3857–3869.
Sugimoto-Shirasu,K., Stacey,N.J., Corsar,J., Roberts,K. and McCann,M.C. (2002) DNA topoisomerase VI is essential for endoreduplication in *Arabidopsis*. *Curr. Biol.*, **12**, 1782–1786.
Tingey,A.P. and Maxwell,A. (1996) Probing the role of the ATP-operated clamp in the Strand-passage reaction of DNA gyrase. *Nucleic Acids Res.*, **24**, 4868–4873.
Van Duyne,G.D., Standaert,R.F., Karplus,P.A., Schreiber,S.L. and Clardy,J. (1993) Atomic structures of the human immunophilin FKBP-12 complexes with FK506 and rapamycin. *J. Mol. Biol.*, **229**, 105–124.
Wang,J.C. (1996) DNA topoisomerases. *Annu. Rev. Biochem.*, **65**, 635–692.
Wang,J.C. (2002) Cellular roles of topoisomerases: a molecular perspective. *Nat. Rev. Mol. Cell Biol.*, **3**, 430–440.
Wigley,D.B., Davies,G.J., Dodson,E.J., Maxwell,A. and Dodson,G. (1991) Crystal structure of an amino-terminal fragment of the DNA gyrase B protein. *Nature*, **351**, 624–629.
Winn,M.D., Isupov,M.N. and Murshudov,G.N. (2001) Use of TLS parameters to model anisotropic displacements in macromolecular refinement. *Acta Crystallogr. D*, **57**, 122–133.
Yin,Y., Cheong,H., Friedrichsen,D., Zhao,Y., Hu,J., Mora-Garcia,S. and Chory,J. (2002) A crucial role for the putative *Arabidopsis* topoisomerase VI in plant growth and development. *Proc. Natl Acad. Sci. USA*, **99**, 10191–10196.
Zharkov,D.O., Golan,G., Gilboa,R., Fernandes,A.S., Gerchman,S.E., Kycia,J.H., Rieger,R.A., Grollman,A.P. and Shoham,G. (2002) Structural analysis of an *Escherichia coli* endonuclease VIII covalent reaction intermediate. *EMBO J.*, **21**, 789–800.

Received September 20, 2002;
revised and accepted November 4, 2002